NASA Technical Memorandum 4038

Computer Program for Parameterization of Nucleus-Nucleus Electromagnetic Dissociation Cross Sections

John W. Norbury, Lawrence W. Townsend,
and Forooz F. Badavi

JUNE 1988

NASA

NASA Technical Memorandum 4038

Computer Program for Parameterization of Nucleus-Nucleus Electromagnetic Dissociation Cross Sections

John W. Norbury
University of Idaho
Moscow, Idaho

Lawrence W. Townsend
Langley Research Center
Hampton, Virginia

Forooz F. Badavi
Planning Research Corporation
Hampton, Virginia

National Aeronautics
and Space Administration

**Scientific and Technical
Information Division**

1988

Symbols

A	nucleon number
d	overlap distance, fm
EM	electromagnetic
$E_{\mathrm{photonmax}}$	maximum photon energy, MeV
GDR	giant dipole resonance
g_n	neutron branching ratio
g_p	proton branching ratio
N_{pts}	number of integration intervals
$R_{0.1}$	10-percent-charge density radius, fm
T_{th}	threshold energy, MeV
Z	proton number
Γ	GDR width, MeV
σ_{EM}	electromagnetic dissociation cross section, mb

Introduction

As the United States space program heads toward the era of permanent occupation of the near-Earth environment via the habitation of a permanent Space Station, the problem of protection of astronauts from the harmful effects of cosmic radiation assumes greater and greater importance. Of special concern are the effects of galactic cosmic rays in the form of relativistic nuclei (ref. 1). When a relativistic nucleus impinges upon a spacecraft wall, it undergoes several reactions, an important one of which is fragmentation, whereby the nucleus breaks up into smaller pieces which subsequently decay. It is these secondary particles which contribute to the radiation environment inside a spacecraft. The problem of fragmentation of relativistic nuclei is the subject of a continuing research effort by the present authors and others (ref. 2). An alternative mechanism, which can produce the same sort of radiation environment as the fragmentation mechanism, is that of electromagnetic dissociation by which the electromagnetic field of one nucleus excites states in another nucleus which subsequently decay. Norbury and Townsend have led a study (ref. 3) of the significance of this mechanism to galactic heavy ion break up and have concluded that it is of major importance (i.e., large cross section) for the removal of a few nucleons when a relativistic nucleus impinges upon a spacecraft wall. Consequently, the mechanism of the electromagnetic dissociation *must* be included when one is trying to predict the radiation environment in the interior of a spacecraft when the exterior environment is composed of galactic heavy ions.

In the present work, it is assumed that the photonuclear cross section is totally dominated by the giant dipole resonance (GDR) (refs. 4 through 9) and, furthermore, that the GDR decays only via single nucleon emission.

Parameterizations

The theoretical formulations of electromagnetic (EM) dissociation cross sections (ref. 3) are certainly adequate as they stand. However, because of the large number of parameters that need to be input "by hand" into the EM code (ref. 3) in an interactive session, one cannot use the EM code as an integral part of a heavy ion transport code. Thus, parameterizations are provided for the giant dipole resonance width Γ, the 10-percent-charge density radius $R_{0.1}$, the photoneutron and photoproton threshold energies T_{th} and branching ratios g_p and g_n, the nucleus-nucleus overlap distance d, and finally the number of integration intervals used in the numerical integration of the photon spectrum and photonuclear cross section.

An adequate parameterization of all of these quantities means that the only inputs required for the EM code are the projectile kinetic energy and the mass (A) and charge (Z) numbers of the projectile and target.

Giant Dipole Resonance Width

Inspection of table 1 of reference 3 indicates that light nuclei have large widths (of the order of 10 MeV) and heavy nuclei have relatively small widths (around 4–5 MeV). However, attempts to parameterize Γ have not been very successful (ref. 5) as it can be sensitive to nuclear structure effects. Fortunately, the EM cross sections are not very sensitive to Γ (ref. 3), and a very simple parameterization seems to be adequate. Thus, we take

$$\Gamma = 10 \text{ MeV} \qquad (A \leq 50) \qquad (1)$$

$$\Gamma = 4.5 \text{ Mev} \qquad (A \geq 50) \qquad (2)$$

These values are listed for a representative sample of some nuclei in table 1, together with the values from reference 3.

Branching Ratios

Consistent with our assumption that the GDR decays only via single nucleon emission, the neutron branching ratio is

$$g_n = 1 - g_p \qquad (3)$$

where it remains to parameterize g_p, the proton branching ratio. We shall use the one provided by Westfall et al. (ref. 6) as

$$g_p = \text{Min}\,[Z/A, 1.95 \exp(-0.0075Z)] \qquad (4)$$

which denotes the minimum value of the two quantities in brackets. Again these values are listed in table 1.

Photonuclear Reaction Thresholds

The cross section is not strongly dependent upon the particle reaction thresholds; therefore, we use 0.001 MeV to avoid obtaining an infinite value in the EM codes (note that a value of 0 MeV would cause numerical difficulty). However, the true value is on the order of 10 MeV (see table 2), and one would therefore think that this would be a poor approximation, especially as the dominant contribution to the virtual photon spectrum occurs at low energy. This effect is offset due to the giant dipole cross section becoming negligible near the threshold and therefore contributing nothing to the total EM cross section. As a result of

$$T_{\mathrm{th}} = 0.001 \text{ MeV} \tag{5}$$

(see table 2), the code now no longer requires nuclear mass excesses as input; this is a considerable improvement in simplicity.

10-Percent-Charge Density Radius

Nuclear radii are well parameterized by $1.18A^{1/3}$ fm. Motivated by this result, we investigated the possibility of adding a constant to this form in order to fit the 10-percent-charge density radii. (See table 3 of ref. 3.) The best fit was obtained with

$$R_{0.1} = 1.18A^{1/3} + 0.75 \text{ fm} \tag{6}$$

and the results are listed in table 3, together with the results of reference 3 where a variety of complicated models were used to calculate $R_{0.1}$. As can be seen, equation (6) reproduces the 10-percent-charge radii very accurately.

Overlap Distance

The nucleus-nucleus overlap distance was chosen as

$$d = 0 \text{ fm} \tag{7}$$

Integration Variables

The simple trapezoidal rule was used in the numerical integration. A very reliable result can be obtained with the number of integration intervals being

$$N_{\mathrm{pts}} = 50 \tag{8}$$

Furthermore, just as the lower limit in energy is taken as 0.001 MeV, inspection of figures 10 through 30 of reference 3 indicates that an upper energy limit

$$E_{\mathrm{photonmax}} = 70 \text{ MeV} \tag{9}$$

is sufficient to cover the entire GDR region. The reader is reminded that the relatively small value used in equation (9) results from the dynamics of the GDR and is not strongly dependent upon the incident kinetic energy of the projectile.

Results

Equations (1) through (9) summarize *all* the parameterizations of the nucleus-nucleus EM dissociation cross sections. The only required inputs to the new EM code (see listing in the appendix) are the projectile kinetic energy and the charge and mass numbers of the projectile and target.

The theoretical (ref. 3) and experimental GDR photonuclear reaction cross sections (refs. 5, 10, and 11), which appear in figures 1 through 13, are presented with these parameterizations. The comparison between the present work and that of reference 3 is quite good except for ^{58}Ni and ^{54}Fe. The case of ^{54}Fe is particularly bad because the present parameterization of g_p leads to poor results for nuclei far from stability. We shall return to this point later.

The total nucleus-nucleus EM dissociation cross sections are presented in tables 4 through 8. (Note that table 7 presents results for target fragmentation, whereas all the other results are for projectile fragmentation. To calculate target fragmentation with the code in the appendix, one should simply swap the projectile and target.) Also included in these tables are the calculations of reference 3. Experimental data (refs. 7, 8, and 9) are also included in tables 5, 6, and 7.

The agreement between the parameterization of σ_{EM} and the data is reasonably good. However, generally the parameterization gives a larger result than the projectile fragmentation data of tables 5 and 6 and a smaller result than the target fragmentation data of table 7. The reason for this is that the parameters were adjusted to give the best overall agreement with the data. Note however, that the errors associated with the data are very large. The errors in the data of Heckman and Lindstrom (ref. 7) in table 5 are typically 50 percent and those of Mercier et al. (ref. 9) in table 7 are around 25 percent. Thus, even though our parameterization agrees with the data usually within 20 percent, this very large uncertainty in the data means that the parameterizations are really as uncertain as the data. Therefore, there is a very urgent need for more accurate data.

The ^{18}O (ref. 8) in table 6 has very small errors, and our parameterization typically overestimates the data. There are two reasons for this. First, the photonuclear cross section (figs. 10 and 11) displays features very different from the normal giant dipole resonance. Thus, any attempt to fit the standard GDR is bound to fail. Second, the parameterization of the branching ratio in equation (4) is most accurate for stable nuclei. For unstable nuclei like ^{18}O and ^{54}Fe (refer to earlier discussion), its accuracy is limited. Fortunately, however, the production cross section of these rare nuclei is reasonably small, and the corresponding inaccuracy will not manifest itself as a large inaccuracy in a transport code. Nevertheless, a good description of the electromagnetic cross sections for unstable nuclei would be valuable.

Finally, as seen from tables 4 through 8, agreement between our parameterizations and the results of reference 3 is excellent.

Concluding Remarks and Future Needs

The parameterizations presented herein are able to match the experimental data to within the uncertainty of the data. This work has demonstrated that the following points need to be further addressed (in order of importance):

1. Much more accurate data are needed
2. A more accurate theoretical model is needed to describe the photonuclear reaction cross sections; this would consequently improve the parameterizations
3. A better description of unstable nuclei (such as ^{18}O and ^{54}Fe) is needed, particularly the branching ratios and photonuclear cross sections
4. Multiple nucleon emission should be included
5. Alternatives to the Weizsäcker-Williams method for obtaining the photon spectrum should be investigated
6. The size of the interference between the strong and electromagnetic forces needs to be determined (we have assumed that it is zero (refs. 8 and 12))
7. Multipolarities other than electric dipole need to be included (refs. 12 and 13)
8. Curvilinear, rather than straight-line, trajectories should be considered (refs. 12 and 13)

NASA Langley Research Center
Hampton, Virginia 23665-5225
May 4, 1988

Appendix

Computer Code

The computer program of reference 3 has been modified to include the parameterizations of the present work. The only required inputs are the projectile kinetic energy and the projectile and target mass and charge numbers. At the end of the program, a sample output is provided.

Program Listing

```
10    REM               COULOMB PARAMETERIZATION
20    REM               ----------------------
30    REM               ----------------------
40    REM
50                                         FIXED 2
60    REM
70    REM
80              DIM Ephoton(900)
90              DIM Sigmanu(900)
100             DIM Ne(900)
110   REM
120   REM
130   REM Fsc = Fine Structure Constant
140   Fsc=1/137.03604
150   Hbarc=197.32858
160   Mncsq=938.95
170   Mneutron=939.5731
180   Mproton=938.2796
190   Amu=931.5016
200   Mstar=.7*Mncsq
210   J=36.8
220   Q=17
230   Epsilon=.0768
240   INPUT "ENTER Z OF TARGET",Zt
250   INPUT "ENTER A OF TARGET",At
260   Nt=At-Zt
270   INPUT "ENTER Z OF PROJECTILE",Zp
280   INPUT "ENTER A OF PROJECTILE",Ap
290   Np=Ap-Zp
300   IF Ap<50 THEN Width=10.0
310   IF Ap>=50 THEN Width=4.5
320   Frac1=1.95*EXP(-.075*Zp)
330   Frac2=Zp/Ap
340   IF Frac1<=Frac2 THEN Fracproton=Frac1
350   IF Frac2<Frac1 THEN Fracproton=Frac2
360   R10t=1.18*At^(1/3)+.75
370   R10p=1.18*Ap^(1/3)+.75
380   Dee=0
390     Bmin=R10t+R10p-Dee
400   INPUT "WHAT IS KE/N OF PROJECTILE  (MeV/N) ?",Tlab
410   Gamma=1+Tlab/Mncsq
420   Vel=SQR(1-1/Gamma^2)
430     REM Gamma IS THE RELATIVISTIC GAMMA FACTOR OF PROJ
440     REM Vel   IS VELOCITY OF PROJ IN UNITS OF C  (RELATIVISTIC BETA FACTOR)
450   Sigmam=120*Np*Zp/(PI*Ap*Width)
460   Ro=1.18*Ap^(1/3)
470   U=3*J*Ap^(-1/3)/Q
480   Egdr=SQR(8.0*J*Hbarc^2/(Mstar*Ro^2)*1/(1+U-(1+Epsilon+3*U)*Epsilon/(1+Epsi
lon+U)))
490   REM
500   REM   NUMERICAL INTEGRATION OR PLOT
510   REM
```

```
520       Ephoton(1)=.001
530    REM  IF Ethreshgn>Ethreshgp THEN Ephoton(1)=Ethreshgp
540    Ephotonmax=70
550    Npts=50
560    REM
570    REM  Eint is defined as the integration or plot interval
580    REM
590         Eint=(Ephotonmax-Ephoton(1))/(Npts-1)
600         Sum=0
610         Sump=0
620         Sumn=0
630    REM
640    REM
650    REM
660     FOR I=1 TO Npts
670       Ephoton=Ephoton(1)+(I-1)*Eint
680                   Ephoton(I)=Ephoton
690       Sigmanu=Sigmam/(1+(Ephoton^2-Egdr^2)^2/(Ephoton^2*Width^2))
700                   Sigmanu(I)=Sigmanu
710       Ecutoff=Hbarc*Gamma*Vel/Bmin
720       G=Ephoton/Ecutoff
730       CALL Bessel(G,K0,K1)
740       Ne=2*Zt^2*Fsc/(Ephoton*PI*Vel^2)*(G*K0*K1-.5*Vel^2*G^2*(K1^2-K0^2))
750                   Ne(I)=Ne
760        Function=Sigmanu*Ne
770        IF I=1 THEN Function=.5*Function
780        IF I=Npts THEN Function=.5*Function
790        Sum=Sum+Function
800            Functionp=Fracproton*Function
810            Functionn=(1-Fracproton)*Function
820            IF Ephoton<Ethreshgp THEN Functionp=0
830            IF Ephoton<Ethreshgn THEN Functionn=0
840            Sump=Sump+Functionp
850            Sumn=Sumn+Functionn
860     NEXT I
870    REM
880    REM
890    REM
900         Integralp=Eint*Sump
910         Integraln=Eint*Sumn
920         Integral=Integralp+Integraln
930    IF Ephotonmax-Egdr<40 THEN PRINT "WARNING: increase Ephotonmax"
940         PRINT
950    PRINT
960    PRINT "Width (MeV)",Width
970    PRINT "Zt",Zt
980    PRINT "At",At
990    PRINT "Zp",Zp
1000   PRINT "Ap",Ap
1010   PRINT "KE/N (MeV/N)",Tlab
1020   PRINT
1030   PRINT
1040   PRINT
1050   PRINT "Lower limit of integration (MeV)",Ephoton(1)
1060   PRINT "Upper limit of integration (MeV)",Ephotonmax
1070   PRINT "Number of integration intervals is",Npts
1080   PRINT "Value of integration interval width (MeV)",Eint
1090   PRINT
1100   PRINT
1110   PRINT "Sigmanu (mb)",Sigmanu
1120   PRINT "Sigmam (mb)",Sigmam
1130   PRINT "Ro (fm)",Ro
```

```
1140  PRINT "U",U
1150  PRINT "GDR Energy (MeV)",Egdr
1160  PRINT
1170  PRINT
1180  PRINT
1190  PRINT "PROJ VELOCITY (=Beta factor)-units of c",Vel
1200  PRINT "RELATIVISTIC GAMMA FACTOR OF PROJ (MeV/N)",Gamma
1210  PRINT "Ecutoff  (MeV)",Ecutoff
1220  PRINT "10 percent charge radius of target  (fm)    ",R10t
1230  PRINT "10 percent charge radius of projectile  (fm)",R10p
1240  PRINT "Dee",Dee
1250  PRINT "Bmin  (fm)",Bmin
1260  PRINT
1270  PRINT
1280  PRINT
1290  PRINT "COULOMB DISSOCIATION CROSS SECTION (Sigmaww)  (mb)",Integral
1300  PRINT
1310  PRINT "Sigma(gamma,p)   (mb)",Integralp
1320  PRINT "Sigma(gamma,n)   (mb)",Integraln
1330  STOP
1340  END
1350     SUB Bessel(G,K0,K1)
1360      A1=3.5156229
1370      A2=3.0899424
1380      A3=1.2067492
1390      A4=.2659732
1400      A5=.0360768
1410      A6=.0045813
1420      A7=.39894228
1430      A8=.01328592
1440      A9=.00225319
1450     A10=.00157565
1460     A11=.00916281
1470     A12=.02057706
1480     A13=.02635537
1490     A14=.01647633
1500     A15=.00392377
1510     A16=.87890594
1520     A17=.51498869
1530     A18=.15084934
1540     A19=.02658733
1550     A20=.00301532
1560     A21=.00032411
1570     A22=.39894228
1580     A23=.03988024
1590     A24=.00362018
1600     A25=.00163801
1610     A26=.01031555
1620     A27=.02282967
1630     A28=.02895312
1640     A29=.01787654
1650     A30=.00420059
1660      B1=.57721566
1670      B2=.42278420
1680      B3=.23069756
1690      B4=.0348859
1700      B5=.00262698
1710      B6=.0001075
1720      B7=.0000074
1730      B8=1.25331414
1740      B9=.07832358
1750     B10=.02189568
```

ORIGINAL PAGE IS
OF POOR QUALITY

```
1760      B11=.01062446
1770      B12=.00587872
1780      B13=.00251540
1790      B14=.00053208
1800      B15=.15443144
1810      B16=.67278579
1820      B17=.18156897
1830      B18=.01919402
1840      B19=.00110404
1850      B20=.00004686
1860      B21=1.25331414
1870      B22=.23498619
1880      B23=.03655620
1890      B24=.01504268
1900      B25=.00780353
1910      B26=.00325614
1920      B27=.00068245
1930   T=G/3.75
1940   IF G<=3.75 THEN I0=1+A1*T^2+A2*T^4+A3*T^6+A4*T^8+A5*T^10+A6*T^12
1950   IF G>3.75 THEN I0=1/SQR(G)*EXP(G)*(A7+A8/T+A9/T^2-A10/T^3+A11/T^4-A12/T^5+
A13/T^6-A14/T^7+A15/T^8)
1960   IF G<=3.75 THEN I1=G*(.5+A16*T^2+A17*T^4+A18*T^6+A19*T^8+A20*T^10+A21*T^12
)
1970   IF G>3.75 THEN I1=1/SQR(G)*EXP(G)*(A22-A23/T-A24/T^2+A25/T^3-A26/T^4+A27/T
^5-A28/T^6+A29/T^7-A30/T^8)
1980   S=G/2
1990   IF G<=2 THEN K0=-LOG(S)*I0-B1+B2*S^2+B3*S^4+B4*S^6+B5*S^8+B6*S^10+B7*S^12
2000   IF G>2 THEN K0=1/SQR(G)*EXP(-G)*(B8-B9/S+B10/S^2-B11/S^3+B12/S^4-B13/S^5+B
14/S^6)
2010   IF G<=2 THEN K1=LOG(S)*I1+1/G*(1+B15*S^2-B16*S^4-B17*S^6-B18*S^8-B19*S^10-
B20*S^12)
2020   IF G>2 THEN K1=1/SQR(G)*EXP(-G)*(B21+B22/S-B23/S^2+B24/S^3-B25/S^4+B26/S^5
-B27/S^6)
2030   SUBEND
```

Sample Output

```
Width (MeV)             4.50
Zt                      82.00
At                      208.00
Zp                      26.00
Ap                      56.00
KE/N (MeV/N)            1880.00


Lower limit of integration (MeV)         .00
Upper limit of integration (MeV)         70.00
Number of integration intervals is       50.00
Value of integration interval width (MeV)                   1.43


Sigmanu (mb)            .56
Sigmam (mb)             118.23
Ro (fm)                 4.51
U                       1.70
GDR Energy (MeV)        18.40


PROJ VELOCITY (=Beta factor)-units of c  .94
RELATIVISTIC GAMMA FACTOR OF PROJ (MeV/N)                   3.00
Ecutoff  (MeV)          42.95
10 percent charge radius of target  (fm)                    7.74
10 percent charge radius of projectile  (fm)                5.26
Dee                     0.00
Bmin  (fm)              13.01


COULOMB DISSOCIATION CROSS SECTION (Sigmaww)  (mb)          1020.04

Sigma(gamma,p)   (mb)                    283.00
Sigma(gamma,n)   (mb)                    737.05
```

References

1. Todd, Paul: Unique Biological Aspects of Radiation Hazards—An Overview. *Adv. Space Res.*, vol. 3, no. 8, 1983, pp. 187–194.
2. Townsend, L. W.; Wilson, J. W.; and Norbury, J. W.: A Simplified Optical Model Description of Heavy Ion Fragmentation. *Canadian J. Phys.*, vol. 63, no. 2, Feb. 1985, pp. 135–138.
3. Norbury, John W.; and Townsend, Lawrence W.: *Electromagnetic Dissociation Effects in Galactic Heavy-Ion Fragmentation.* NASA TP-2527, 1986.
4. Spicer, B. M.: The Giant Dipole Resonance. *Advances in Nuclear Physics, Volume 2,* Michel Baranger and Erich Vogt, eds., Plenum Press, Inc., 1969, pp. 1–78.
5. Berman, B. L.; and Fultz, S. C.: Measurements of the Giant Dipole Resonance With Monoenergetic Photons. *Reviews Modern Phys.*, vol. 47, no. 3, July 1975, pp. 713–761.
6. Westfall, G. D.; Wilson, Lance W.; Lindstrom, P. J.; Crawford, H. J.; Greiner, D. E.; and Heckman, H. H.: Fragmentation of Relativistic ^{56}Fe. *Phys. Review,* ser. C, vol. 19, no. 4, Apr. 1979, pp. 1309–1323.
7. Heckman, Harry H.; and Lindstrom, Peter J.: Coulomb Dissociation of Relativistic ^{12}C and ^{16}O Nuclei. *Phys. Review Lett.*, vol. 37, no. 1, July 5, 1976, pp. 56–59.
8. Olson, D. L.; Berman, B. L.; Greiner, D. E.; Heckman, H. H.; Lindstrom, P. J.; Westfall, G. D.; and Crawford, H. J.: Electromagnetic Dissociation of Relativistic ^{18}O Nuclei. *Phys. Review,* ser. C, vol. 24, no. 4, Oct. 1981, pp. 1529–1539.
9. Mercier, M. T.; Hill, J. C.; Wohn, F. K.; and Smith, A. R.: Electromagnetic Dissociation of ^{197}Au by Relativistic Heavy Ions. *Phys. Review Lett.,* vol. 52, no. 11, Mar. 12, 1984, pp. 898–901.
10. Woodworth, J. G.; McNeill, K. G.; Jury, J. W.; Alvarez, R. A.; Berman, B. L.; Faul, D. D.; and Meyer, P.: Photonuclear Cross Sections for ^{18}O. *Phys. Review,* ser. C, vol. 19, no. 5, May 1979, pp. 1667–1683.
11. Norbury, J. W.; Thompson, M. N.; Shoda, K.; and Tsubota, H.: Photoneutron Cross Section of ^{54}Fe. *Australian J. Phys.*, vol. 31, no. 6, Dec. 1978, pp. 471–475.
12. Goldberg, A.: On the Virtual Photon Spectrum for Electromagnetic Dissociation of Relativistic Nuclei in Peripheral Collisions. *Nucl. Phys.*, ser. A, vol. 420, no. 3, June 4, 1984, pp. 636–644.
13. Bertulani, C. A.; and Baur, G.: Electromagnetic Processes in Relativistic Heavy Ion Collisions. *Nucl. Phys.*, ser. A, vol. 458, no. 4, Oct. 20, 1986, pp. 725–744.

Table 1. Resonance Widths and Proton Branching Ratios

Nucleus	Γ, MeV		g_p	
	Reference 3	Present work	Reference 3	Present work
^{7}Li		10.0		0.43
^{9}Be		10.0		0.44
^{12}C	8.0	10.0	0.5	0.5
^{16}O	10.0	10.0	0.5	0.5
^{18}O	12.0	10.0	0.4	0.44
^{20}Ne	10.0	10.0	0.5	0.5
^{28}Si	10.0	10.0	0.5	0.5
^{32}S		10.0		0.5
^{40}Ar	10.0	10.0	0.45	0.45
^{40}Ca	10.0	10.0	0.5	0.44
^{48}Ti		10.0		0.37
^{54}Fe	3.0	4.5	0.7	0.28
^{56}Fe	5.0	4.5	0.28	0.28
^{58}Ni	10.0	4.5	0.5	0.24
^{63}Cu	5.0	4.5	0.28	0.22
^{90}Zr	4.0	4.5	0.05	0.10
^{107}Ag	5.0	4.5	0	0.06
^{106}Gd	4.0	4.5	0	0.02
^{181}Ta		4.5		0.01
^{197}Au	3.5	4.5	0	0.01
^{208}Pb	3.9	4.5	0	0
^{238}U	5.0	4.5	0	0

Table 2. Giant Dipole Resonance Particle Thresholds

Nucleus	Proton threshold, MeV		Neutron threshold, MeV	
	Reference 3	Present work	Reference 3	Present work
^{12}C	15.46	0.001	18.74	0.001
^{16}O	11.62	0.001	15.67	0.001
^{18}O	15.44	0.001	8.05	0.001
^{40}Ar	12.02	0.001	9.87	0.001
^{56}Fe	9.67	0.001	11.20	0.001
^{197}Au	5.27	0.001	8.07	0.001

Table 3. The 10-Percent-Charge Density Radii

Nucleus	10-percent radius, fm	
	Reference 3	Present work
^{7}Li	3.04	3.01
^{9}Be	3.32	3.20
^{12}C	3.33	3.45
^{16}O	3.77	3.72
^{18}O	3.88	3.84
^{20}Ne	4.06	3.95
^{27}Al	4.21	4.29
^{28}Si	4.18	4.33
^{32}S	4.53	4.50
^{40}Ar	4.73	4.79
^{40}Ca	4.80	4.79
^{48}Ti	5.00	5.04
^{54}Fe	5.19	5.21
^{56}Fe	5.28	5.26
^{58}Ni	5.37	5.32
^{64}Cu	5.45	5.47
^{90}Zr	5.90	6.04
^{108}Ag and ^{107}Ag	6.32	6.37
^{160}Gd		7.16
^{181}Ta	7.79	7.42
^{197}Au	7.56	7.62
^{208}Pb	7.83	7.74
^{238}U	8.13	8.06

Table 4. Calculated Total Electromagnetic Absorption Cross Section for 1.88 GeV/N ^{56}Fe Incident Upon Various Targets

Projectile	Energy, GeV/N	Target	σ_{EM}(W), mb (a)	σ_{EM}, mb, for $d = 0$ fm	
				Reference 3	Present work
^{56}Fe	1.88	$^{7}_{3}$Li	2	1.9	2.1
		$^{9}_{4}$Be	3	3.3	3.7
		$^{12}_{6}$C	7	7.3	8.0
		$^{32}_{16}$S	46	46	52
		$^{63}_{29}$Cu	130	140	156
		$^{107}_{47}$Ag	306		377
		$^{181}_{73}$Ta	629	717	830
		$^{208}_{82}$Pb	834	901	1020
		$^{238}_{92}$U	1008	1105	1250

[a]This column represents the isotope-averaged calculations of Westfall et al. (ref. 6).

Table 5. Calculated Total Electromagnetic Reaction Cross Sections for ^{12}C and ^{16}O Incident Upon Various Targets

Projectile	Energy, GeV/N	Target	Final state	σ_{EM}(HL), mb (*a*)	σ_{EM}, mb, for $d = 0$ fm	
					Reference 3	Present work
^{12}C	2.1	^{208}Pb	$^{11}C + n$	50 ± 18	54	68
			$^{11}B + p$	50 ± 25	60	68
	1.05		$^{11}C + n$	38 ± 24	32	43
			$^{11}B + p$	50 ± 26	36	43
^{16}O	2.1		$^{15}O + n$	50 ± 25	78	99
			$^{15}N + p$	97 ± 17	87	26
^{12}C	2.1	^{108}Ag	$^{11}C + n$	22 ± 12	21	26
			$^{11}B + p$	20 ± 12	23	26
	1.05		$^{11}C + n$	22 ± 12	13	17
			$^{11}B + p$	25 ± 20	15	17
^{16}O	2.1		$^{15}O + n$	26 ± 13	30	37
			$^{15}N + p$	29 ± 18	33	37
^{12}C	2.1	^{64}Cu	$^{11}C + n$	10 ± 6	9	11
			$^{11}B + p$	4 ± 8	10	11
	1.05		$^{11}C + n$	10 ± 7	5.9	7.4
			$^{11}B + p$	5 ± 8	6.5	7.4
^{16}O	2.1		$^{15}O + n$	10 ± 7	12.7	16
			$^{15}N + p$	14 ± 9	14	16
^{12}C	2.1	^{27}Al	$^{11}C + n$	0 ± 3	2.1	2.5
			$^{11}B + p$	0 ± 3	2.3	2.5
	1.05		$^{11}C + n$	1 ± 3	1.5	1.8
			$^{11}B + p$	1 ± 3	1.6	1.8
^{16}O	2.1		$^{15}O + n$	0 ± 3	2.9	3.6
			$^{15}N + p$	0 ± 0	3.2	3.6
^{12}C	2.1	^{12}C	$^{11}C + n$	0 ± 1	0.50	0.58
			$^{11}B + p$	0 ± 3	0.54	0.58
	1.05		$^{11}C + n$	0 ± 2	0.36	0.43
			$^{11}B + p$	0 ± 1	0.40	0.43
^{16}O	2.1		$^{15}O + n$	0 ± 2	0.70	0.83
			$^{15}N + p$	0 ± 3	0.76	0.83

[a] This column represents the measurements (isotope averaged) of Heckman and Lindstrom (ref. 7).

Table 6. Calculated Total Electromagnetic Reaction Cross Sections for ^{18}O at 1.7 GeV/N Incident Upon Various Targets

Projectile	Energy, GeV/N	Target	Final state	$\sigma_{EM}(O)$, mb (a)	σ_{EM}, mb, for $d = 0$ fm	
					Reference 3 ($g_p = 0.2$)	Present work
^{18}O	1.7	^{48}Ti	^{17}O + n	8.7 ± 2.7	12	11
			^{17}N + p	0.5 ± 1.0	2	9
		^{208}Pb	^{17}O + n	136 ± 2.9	123	112
			^{17}N + p	20.2 ± 1.8	24	89
		^{238}U	^{17}O + n	140.8 ± 4.1	151	136
			^{17}N + p	2.51 ± 1.6	30	109

[a]This column represents the measurements (isotope averaged) of Olson et al. (ref. 8).

Table 7. Target Fragmentation—Calculated Total Electromagnetic Reaction Cross Sections for Various Projectiles Incident Upon ^{197}Au

Projectile	Energy, GeV/N	Target	Final state	$\sigma_{EM}(M)$, mb (a)	σ_{EM}, mb, for $d = 0$ fm	
					Reference 3	Present work
^{12}C	2.1	^{197}Au	^{196}Au + n	66 ± 20	37	39
^{20}Ne	2.1			136 ± 21	97	104
^{40}Ar	1.8			420 ± 120	278	299
^{56}Fe	1.7			680 ± 160	546	588

[a]This column represents the data of Mercier et al. (ref. 9).

Table 8. Electromagnetic Dissociation Cross Sections for a Variety Of Reactions With $d = 0$ fm

Projectile	Energy	Γ, MeV	g_p	Target	Final state	σ_{EM}, mb, for $d = 0$ fm	
						Reference 3	Present work
^{12}C	86 MeV/N	8.0	0.5	^{12}C	$^{11}C + n$	0.09	0.19
					$^{11}B + p$	0.11	0.19
	350 MeV/N			^{107}Ag	$^{11}C + n$	6	10
					$^{11}B + p$	7	10
	1.05 GeV/N			^{197}Au	$^{11}C + n$	31	41
					$^{11}B + p$	34	41
	2.1 GeV/N			^{197}Au	$^{11}C + n$	53	64
					$^{11}B + p$	57	64
^{16}O	2.1 GeV/N	10.0	0.5	^{9}Be	$^{15}O + n$	0.31	0.38
					$^{15}N + p$	0.34	0.38
				^{12}C	$^{15}O + n$	0.71	0.83
					$^{15}N + p$	0.76	0.83
				^{208}Pb	$^{15}O + n$	80	99
					$^{15}N + p$	87	99
^{40}Ar	213 MeV/N	10.0	0.45	^{12}C	$^{39}Ar + n$	1.2	1.5
					$^{39}Cl + p$	0.9	1.2
^{56}Fe	1.88 GeV/N	5.0	0.28	^{12}C	$^{55}Fe + n$	5.3	5.8
					$^{55}Mn + p$	2.1	2.2
				^{108}Ag	$^{55}Fe + n$	242	272
					$^{55}Mn + p$	97	105
				^{208}Pb	$^{55}Fe + n$	645	737
					$^{55}Mn + p$	258	283
^{238}U	900 MeV/N	5.0	0	^{12}C	$^{237}U + n$	33	36
					$^{237}Pa + p$	0	0.1
				^{27}Al	$^{237}U + n$	142	158
					$^{237}Pa + p$	0	0.3
				^{28}Si	$^{237}U + n$	165	182
					$^{237}Pa + p$	0	0.4
				^{64}Cu	$^{237}U + n$	628	704
					$^{237}Pa + p$	0	1.4
				^{181}Ta	$^{237}U + n$	3208	3760
					$^{237}Pa + p$	0	7.4
				^{208}Pb	$^{237}U + n$	4034	4617
					$^{237}Pa + p$	0	9.1

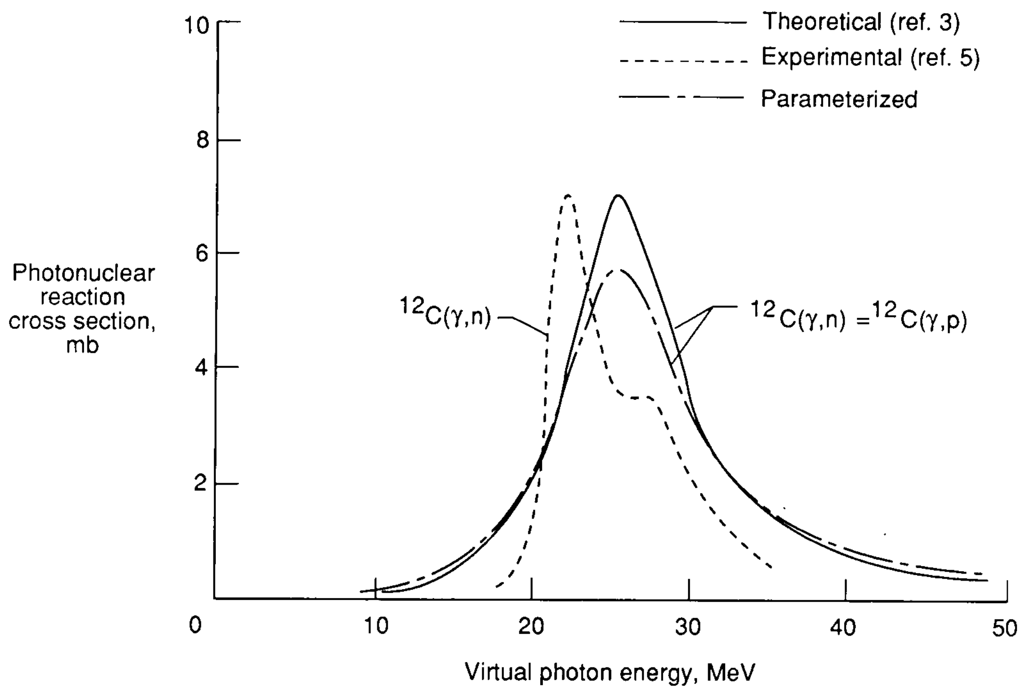

Figure 1. Theoretical, parameterized, and experimental photoneutron reaction cross sections for ^{12}C. Theoretical $\Gamma = 8$ MeV; Parameterized $\Gamma = 10$ MeV; Theoretical g_p = Parameterized $g_p = 0.5$; thus, photoneutron and photoproton cross sections are identical.

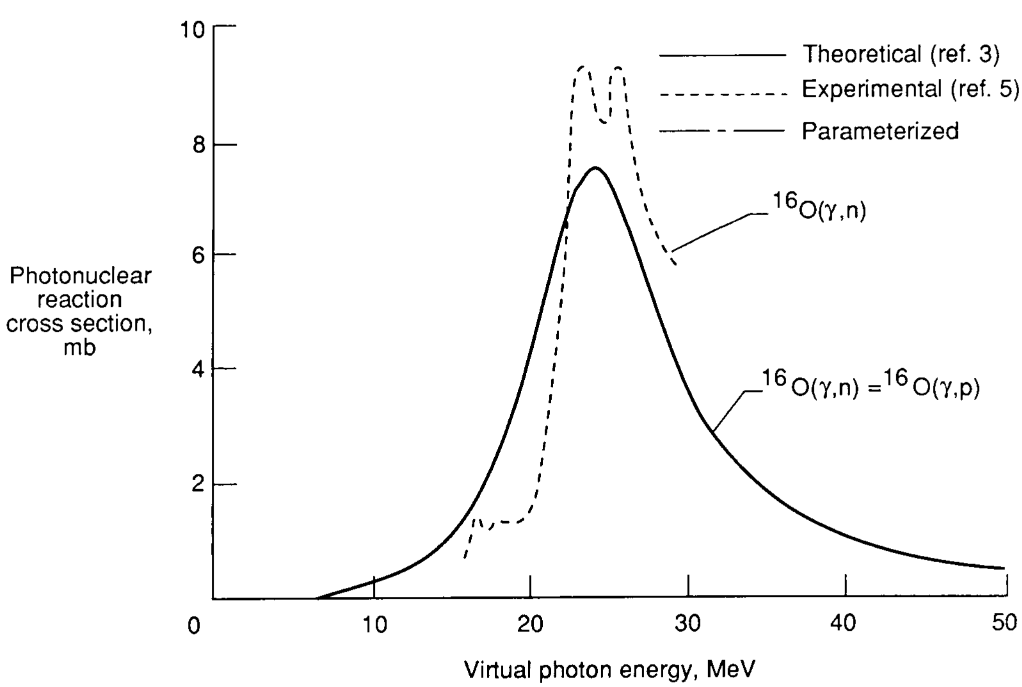

Figure 2. Theoretical, parameterized, and experimental photoneutron reaction cross sections for ^{16}O. $\Gamma = 10$ MeV; Theoretical g_p = Parameterized $g_p = 0.5$; thus, the photoneutron and photoproton cross sections are identical.

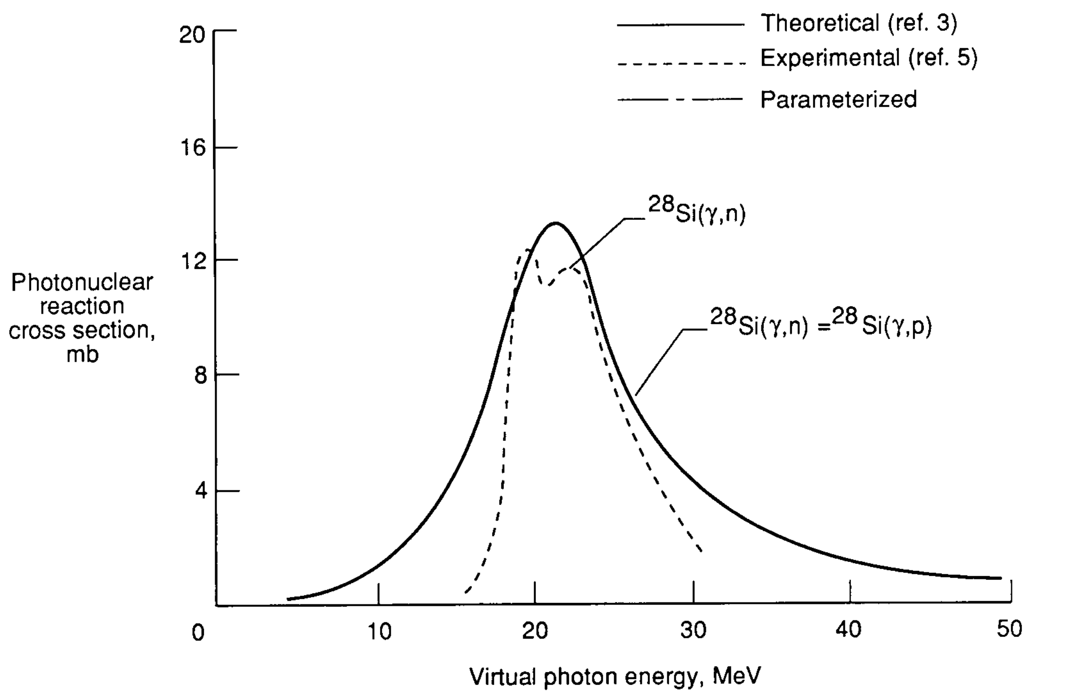

Figure 3. Theoretical, parameterized, and experimental photoneutron reaction cross sections for ^{28}Si. $\Gamma = 10$ MeV; Theoretical g_p = Parameterized $g_p = 0.5$; thus, the photoneutron and photoproton cross sections are identical.

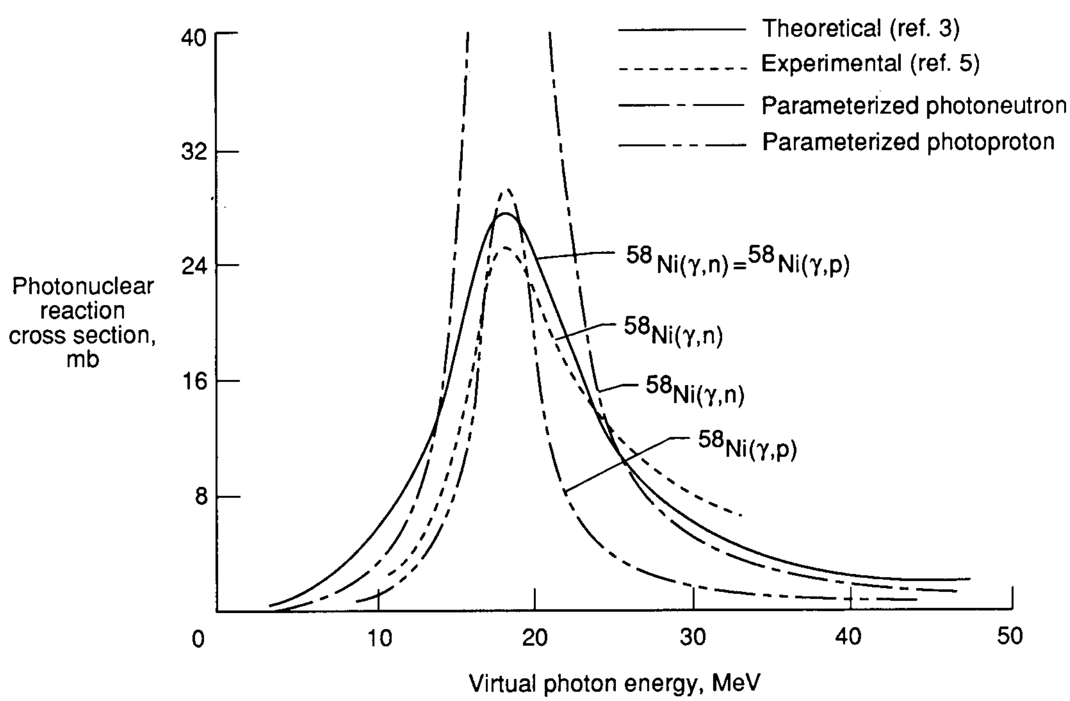

Figure 4. Theoretical, parameterized, and experimental photoneutron reaction cross sections for ^{58}Ni. Theoretical $\Gamma = 10$ MeV; Parameterized $\Gamma = 4.5$ MeV; Theoretical $g_p = 0.5$; thus, the theoretical photoneutron and photoproton cross sections are identical; Parameterized $g_p = 0.24$. Resultant parameterized photoproton cross section is also displayed.

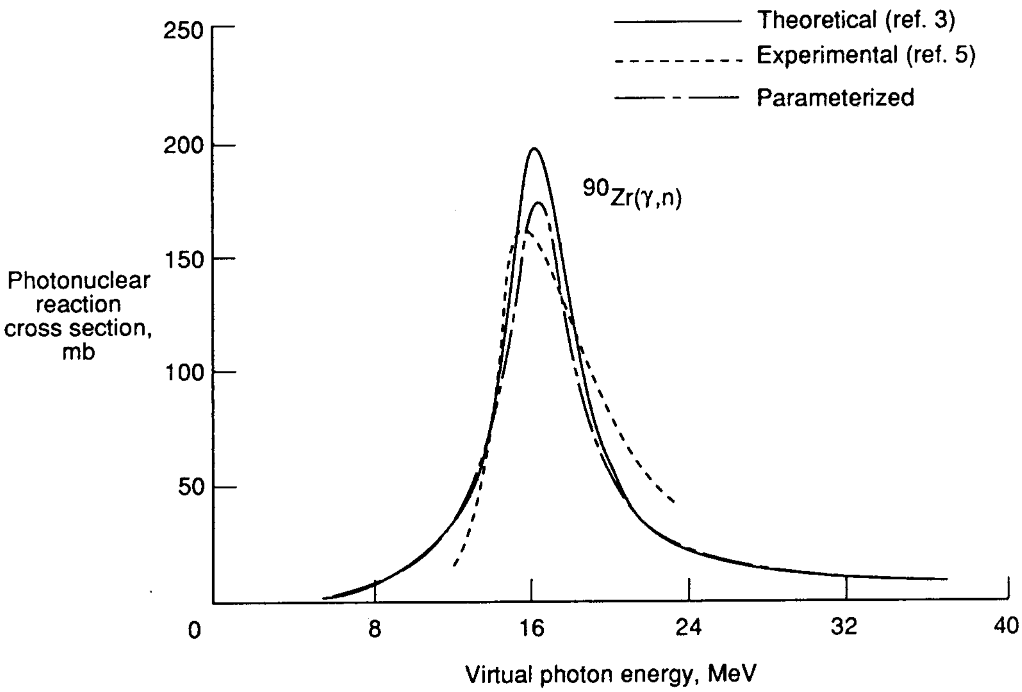

Figure 5. Theoretical, parameterized, and experimental photoneutron reaction cross sections for ^{90}Zr. Theoretical $\Gamma = 4$ MeV; Parameterized $\Gamma = 4.5$ MeV; Theoretical $g_p = 0.05$; Parameterized $g_p = 0.1$.

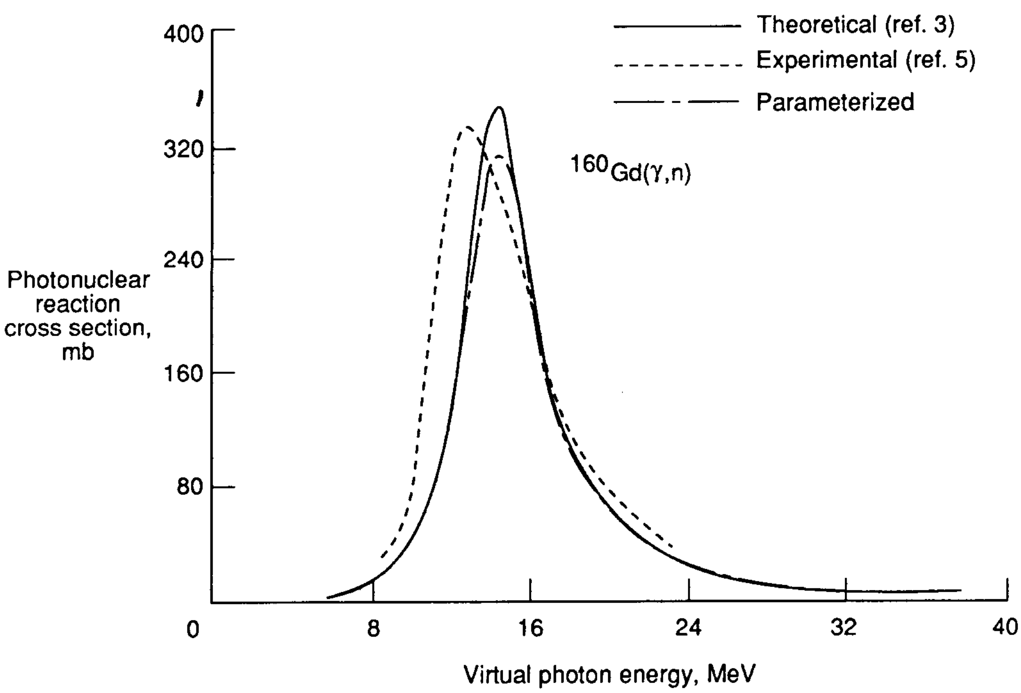

Figure 6. Theoretical, parameterized, and experimental photoneutron reaction cross sections for ^{160}Gd. Theoretical $\Gamma = 4$ MeV; Parameterized $\Gamma = 4.5$ MeV; Theoretical $g_p = 0$; Parameterized $g_p = 0.02$.

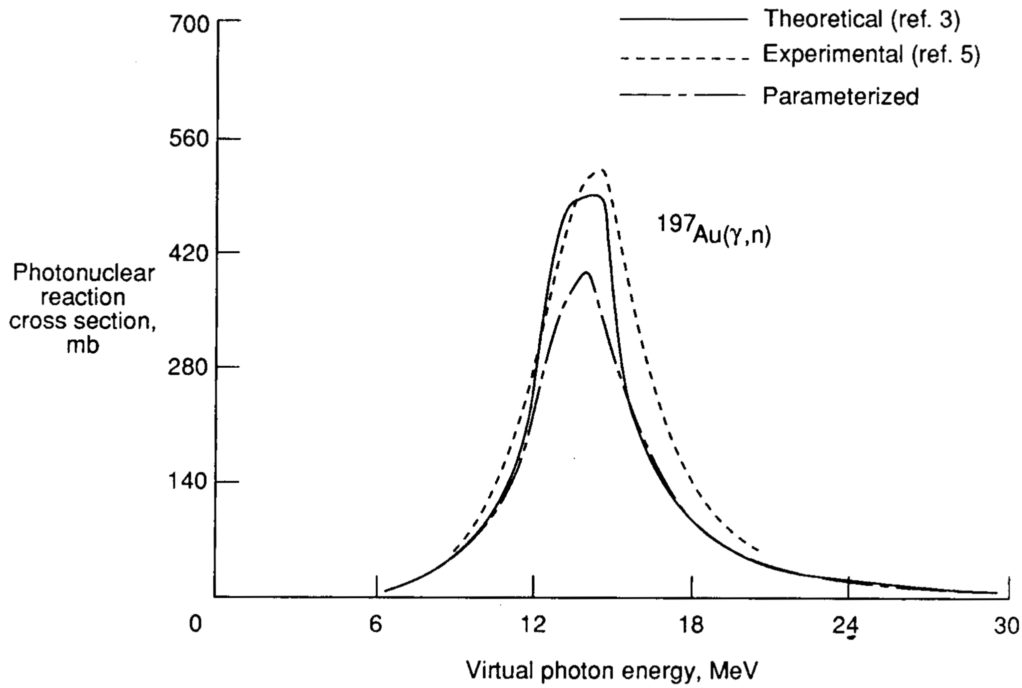

Figure 7. Theoretical, parameterized, and experimental photoneutron reaction cross sections for ^{197}Au. Theoretical $\Gamma = 3.5$ MeV; Parameterized $\Gamma = 4.5$ MeV; Theoretical $g_p = 0$; Parameterized $g_p = 0.01$.

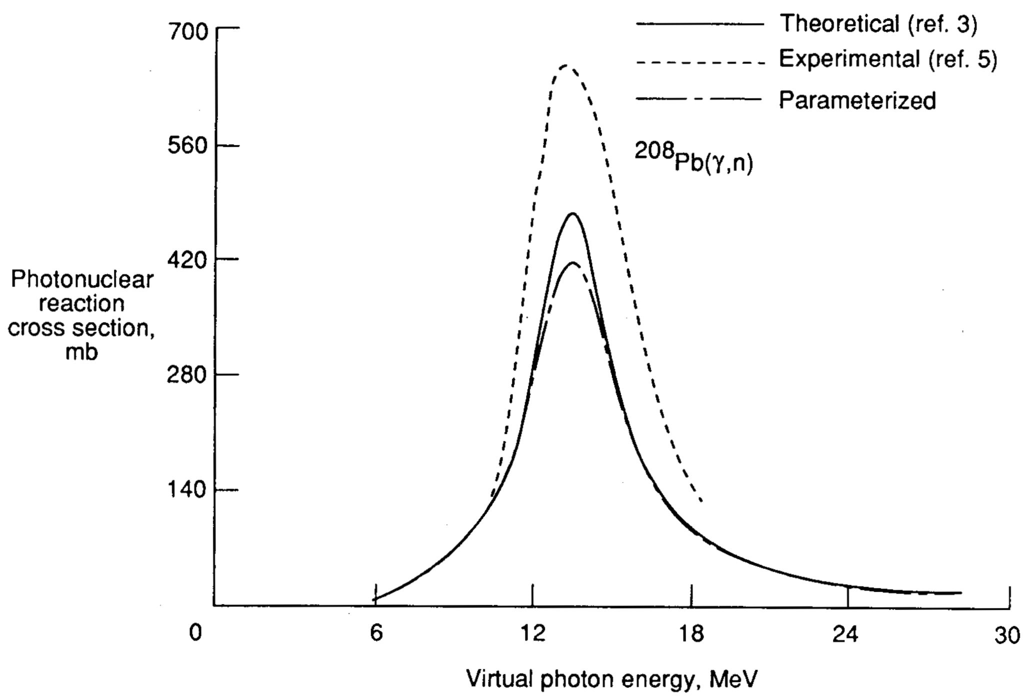

Figure 8. Theoretical, parameterized, and experimental photoneutron reaction cross sections for ^{208}Pb. Theoretical $\Gamma = 3.9$ MeV; Parameterized $\Gamma = 4.5$ MeV; Theoretical g_p = Parameterized $g_p = 0$.

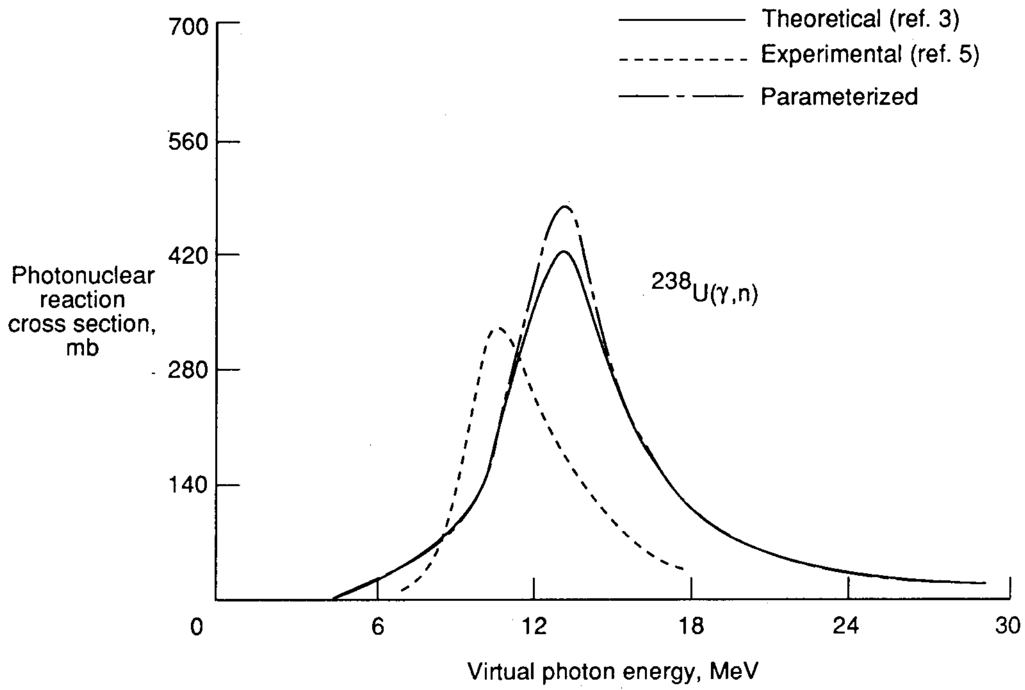

Figure 9. Theoretical, parameterized, and experimental photoneutron reaction cross sections for ^{238}U. Theoretical $\Gamma = 5$ MeV; Parameterized $\Gamma = 4.5$ MeV; Theoretical g_p = Parameterized $g_p = 0$.

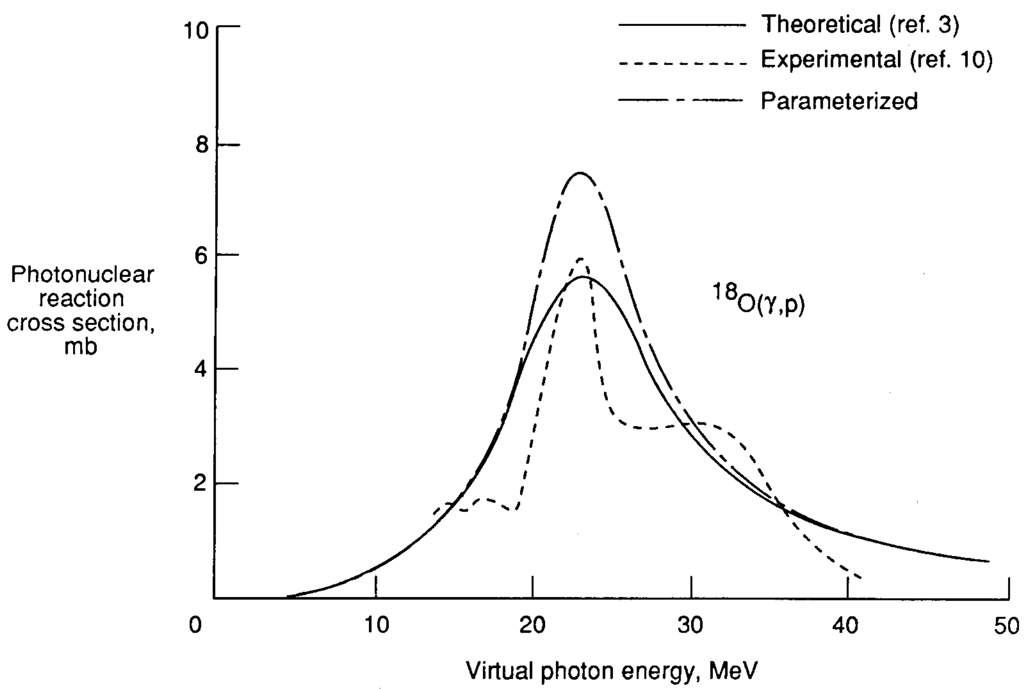

Figure 10. Theoretical, parameterized, and experimental photoproton reaction cross sections for ^{18}O. Theoretical $\Gamma = 12$ MeV; Parameterized $\Gamma = 10$ MeV; Theoretical $g_p = 0.40$; Parameterized $g_p = 0.44$.

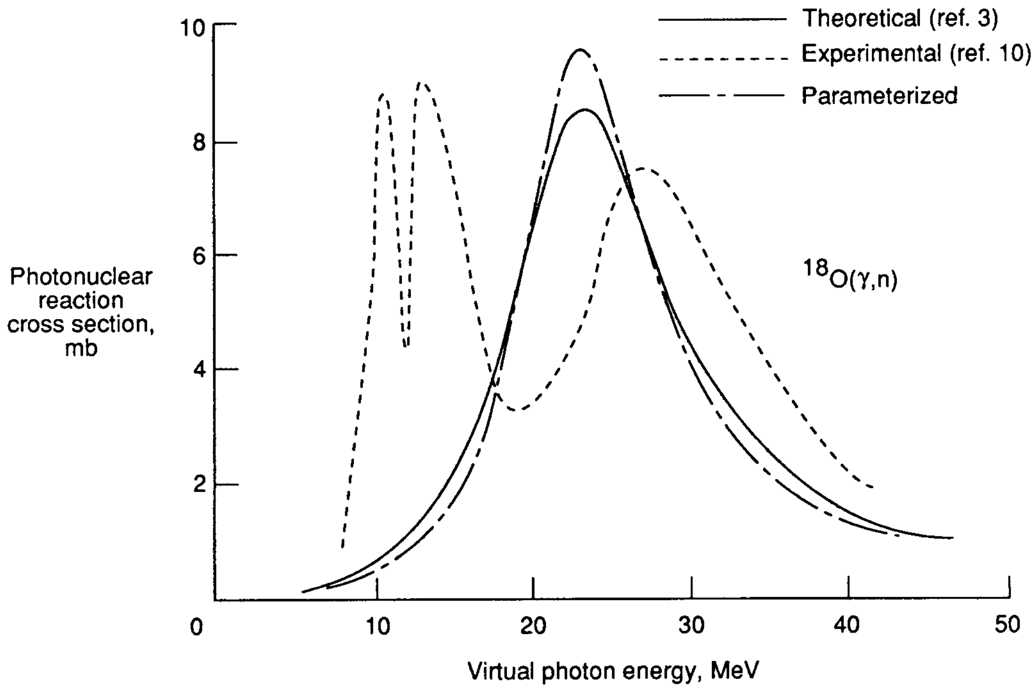

Figure 11. Theoretical, parameterized, and experimental photoneutron reaction cross sections for ^{18}O. Theoretical $\Gamma = 12$ MeV; Parameterized $\Gamma = 10$ MeV; Theoretical $g_n = 0.60$; Parameterized $g_n = 0.56$.

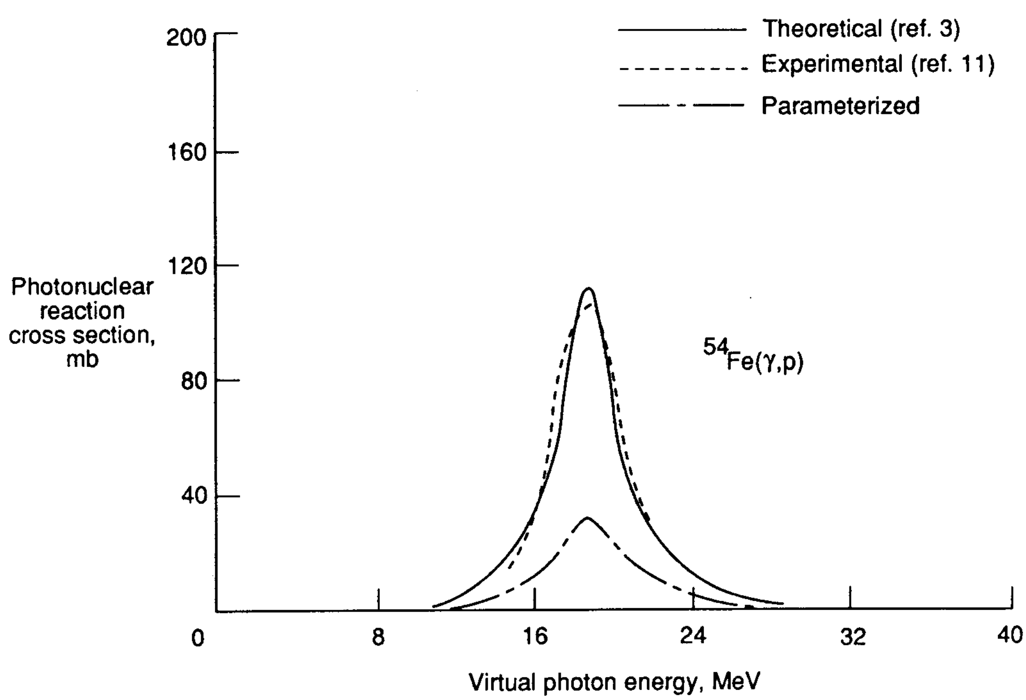

Figure 12. Theoretical, parameterized, and experimental photoproton reaction cross sections for ^{54}Fe. Theoretical $\Gamma = 3$ MeV; Parameterized $\Gamma = 4.5$ MeV; Theoretical $g_p = 0.70$; Parameterized $g_p = 0.28$.

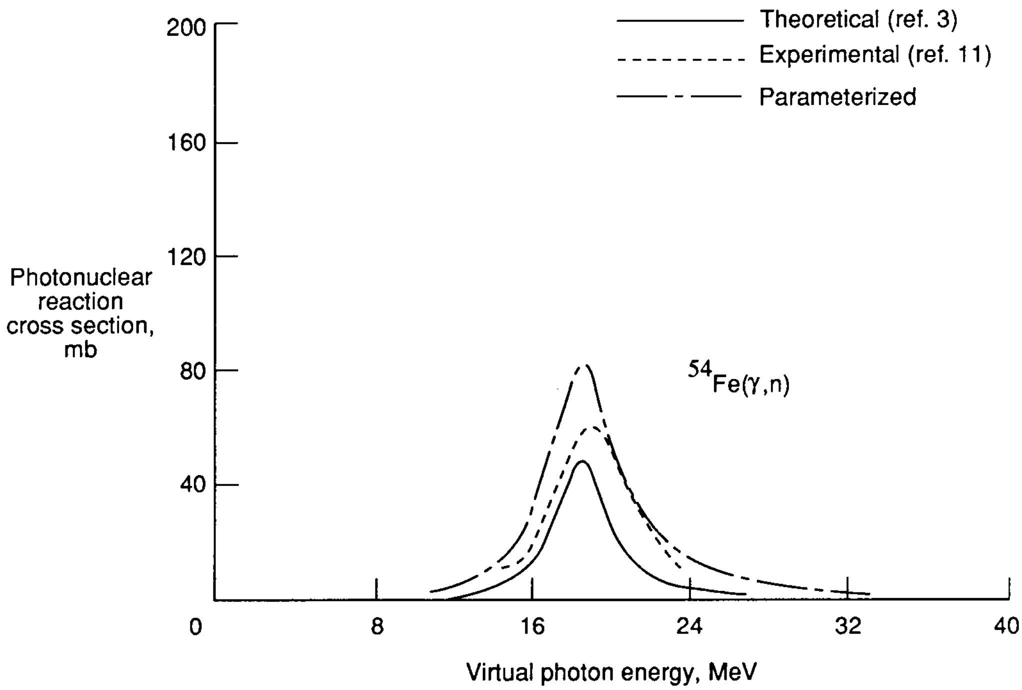

Figure 13. Theoretical, parameterized, and experimental photoneutron reaction cross sections for ^{54}Fe. Theoretical $\Gamma = 3$ MeV; Parameterized $\Gamma = 4.5$ MeV; Theoretical $g_n = 0.30$; Parameterized $g_n = 0.72$.

NASA National Aeronautics and Space Administration

Report Documentation Page

1. Report No.	2. Government Accession No.	3. Recipient's Catalog No.
NASA TM-4038		

4. Title and Subtitle	5. Report Date
Computer Program for Parameterization of Nucleus-Nucleus Electromagnetic Dissociation Cross Sections	June 1988
	6. Performing Organization Code
7. Author(s)	8. Performing Organization Report No.
John W. Norbury, Lawrence W. Townsend, and Forooz F. Badavi	L-16427
9. Performing Organization Name and Address	10. Work Unit No.
NASA Langley Research Center Hampton, VA 23665-5225	199-22-76-01
	11. Contract or Grant No.
12. Sponsoring Agency Name and Address	13. Type of Report and Period Covered
National Aeronautics and Space Administration Washington, DC 20546-0001	Technical Memorandum
	14. Sponsoring Agency Code

15. Supplementary Notes

John W. Norbury: University of Idaho, Moscow, Idaho.
Lawrence W. Townsend: Langley Research Center, Hampton, Virginia.
Forooz F. Badavi: Planning Research Corporation, Hampton, Virginia.

This research was supported in part by NASA Research Cooperative Agreement NCC1-110 with the University of Idaho.

16. Abstract

A computer subroutine parameterization of electromagnetic dissociation cross sections for nucleus-nucleus collisions is presented that is suitable for implementation in a heavy ion transport code. The only inputs required are the projectile kinetic energy and the projectile and target charge and mass numbers.

17. Key Words (Suggested by Authors(s))	18. Distribution Statement
Parameterization Nucleus-nucleus Electromagnetic dissociation Cross sections	Unclassified—Unlimited Subject Category 73

19. Security Classif.(of this report)	20. Security Classif.(of this page)	21. No. of Pages	22. Price
Unclassified	Unclassified	26	A03

NASA-Langley, 1988
For sale by the National Technical Information Service, Springfield, Virginia 22161-2171